

A Proposal for Mach-Zehnder Interferometer

tzachil@rafael.co.il

https://github.com/tzachi012/openEBL-2025-05/blob/main/submissions/EBeam_edXtzachi_38.pdf

1. Introduction

A Mach-Zehnder interferometer (MZI) is the next-level integration building block of passive devices beyond couplers, bringing together two directional or other couplers in cascade. A schematic illustration of an MZI is shown in Fig. 1. The two output ports of the first coupler are linked with the two inputs of the second one. The two connecting waveguides are not necessarily of equal path lengths. In many cases the interferometer is purposely imbalanced, with when path introducing a delay that is longer than that of the other by a difference τ sec. Based on MZI, it is possible to design a very narrow optical filter.

The second part is a brief overview of the theory, the third part presents preliminary simulations, the sixth part presents results and their analysis of a single Mach-Zehnder interferometer and a series of MZIs from the measurements of my design, and the last part presents a summary and conclusions.

2. Theory

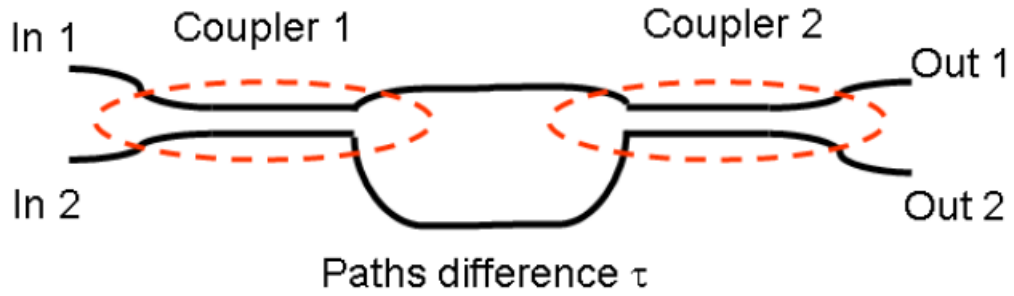


Figure 1: Schematic illustration of a Mach-Zehnder interferometer

The frequency response matrices of a MZI with 50:50 couplers are:

$$(1) \quad T_{MZI}(\omega) = \begin{pmatrix} \sin\left(\frac{1}{2}\omega\tau + \frac{1}{2}\varphi\right) & j\cos\left(\frac{1}{2}\omega\tau + \frac{1}{2}\varphi\right) \\ j\cos\left(\frac{1}{2}\omega\tau + \frac{1}{2}\varphi\right) & \sin\left(\frac{1}{2}\omega\tau + \frac{1}{2}\varphi\right) \end{pmatrix}$$

The transfer of power from input port 1 to output port 1 is $\sin^2\left(\frac{1}{2}\omega\tau + \frac{1}{2}\varphi\right)$, φ is frequency independent phase.

We can cascade 4 such filters with different delays (8τ , 4τ , 2τ , τ) to receive overall narrow optical filter. The transfer of power of cascade MZI filter from input port 1 to output port 1 is $\sin^2\left(\frac{1}{2}\omega 8\tau + \frac{1}{2}\varphi_a\right) \sin^2\left(\frac{1}{2}\omega 4\tau + \frac{1}{2}\varphi_b\right) \sin^2\left(\frac{1}{2}\omega 2\tau + \frac{1}{2}\varphi_c\right) \sin^2\left(\frac{1}{2}\omega\tau + \frac{1}{2}\varphi_d\right)$

A phase shift of π is accumulated over a propagation distance of $\frac{\lambda}{2n_{eff}}$ which is of order of 200nm, it is very difficult to control the fabrication process to such precision. In this work I want to see how the fabrication error affects the filter design.

Stage	Delay	ΔL [nm]
1	8τ	40560
2	4τ	20280
3	2τ	10140
4	τ	5070

Table 1: design parameters.

Expression for effective index, n_{eff} , is a Taylor expression

$$(2) \quad n_{eff} = n_1 + n_2(\lambda - \lambda_0) + n_3(\lambda - \lambda_0)^2$$

3. Modeling and simulation

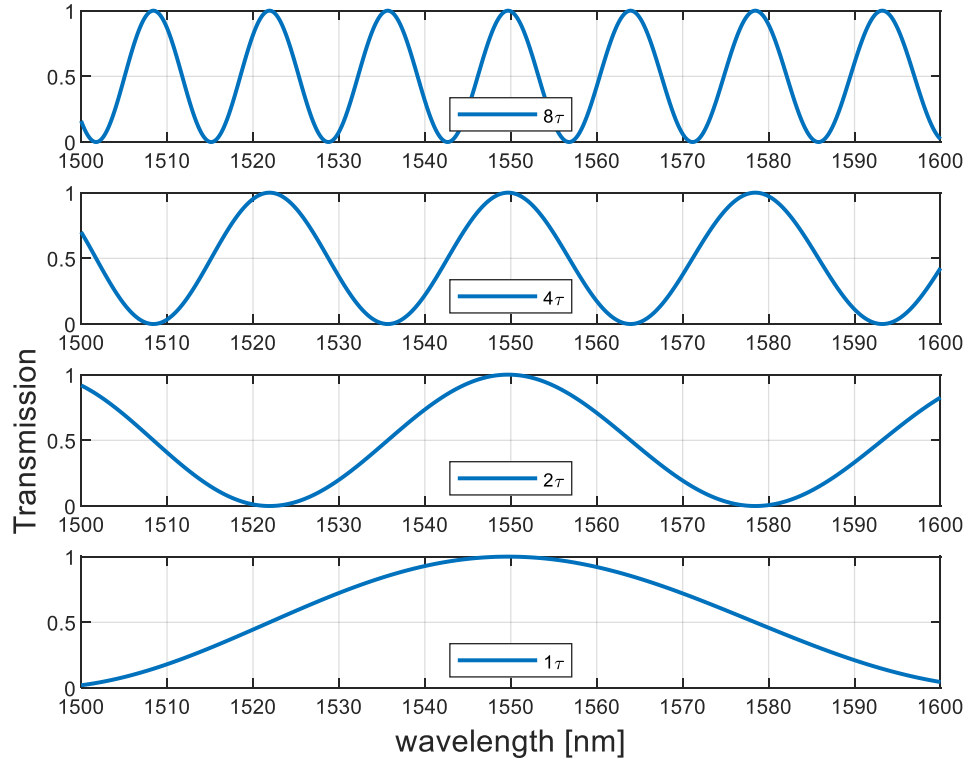


Figure 2: 4 level cascade MZI filter.

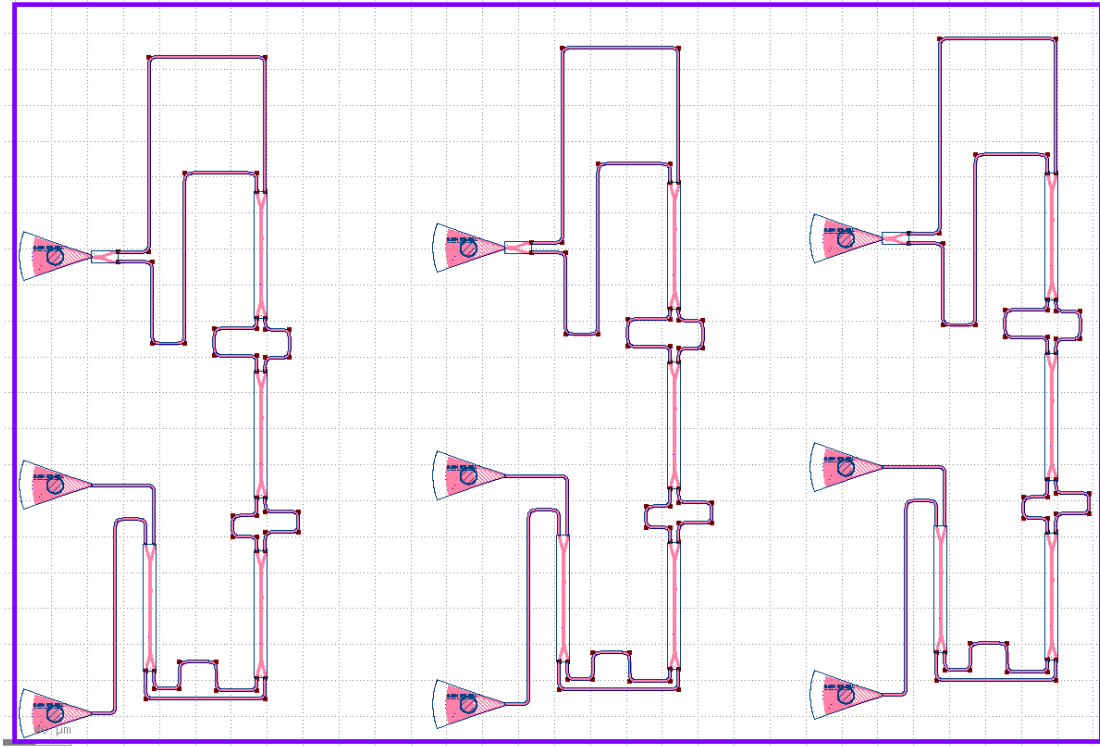


Figure 3: layout of 3 MZI cascade filters of the same design.

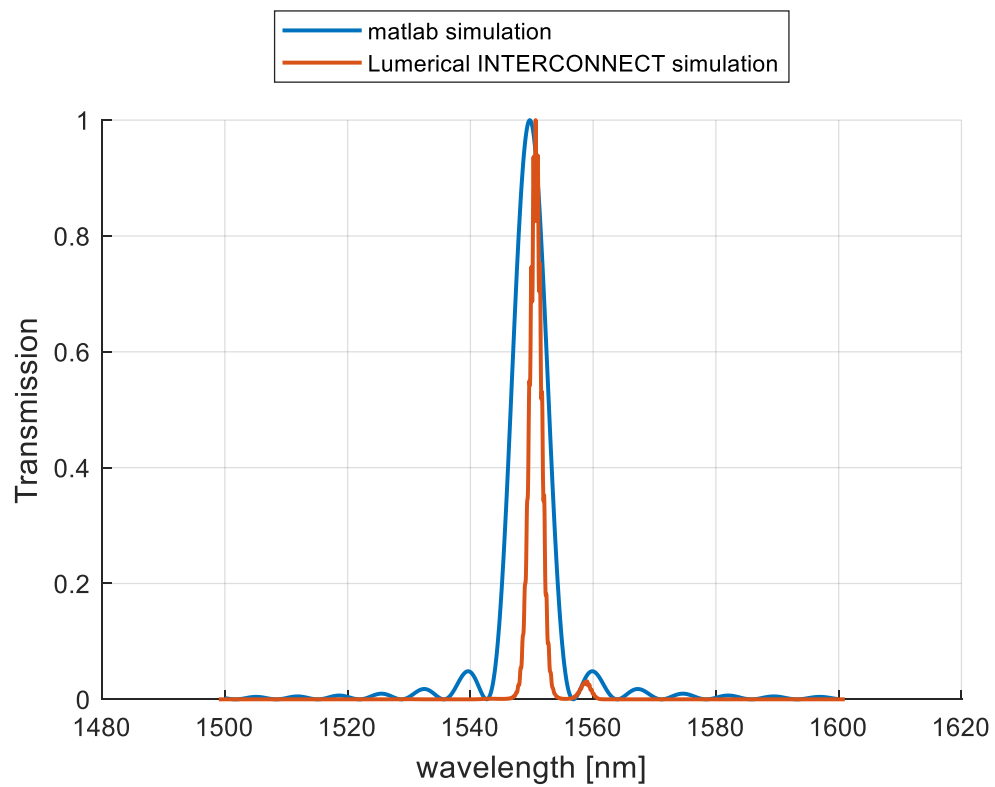


Figure 4: comparison between MATLAB and Lumerical INTERCONNECT simulations, the difference in filter width is due to n_{eff} inaccuracy

4. References

- 4.1. M. Slook et al., "16-channel O-band silicon-photonics wavelength division multiplexer with a 1nm channel spacing", Optics Continuum, Vol. 1, No. 10/15 Oct 2022.
- 4.2. Silicon Photonics (460251). Prof. Avi Zadok, Faculty of Electrical and Computer Engineering, the Technion.
5. Fabrication

The photonic devices were fabricated using the NanoSOI MPW fabrication process by Applied Nanotools Inc. which is based on direct-write 100 keV electron beam lithography technology. Silicon-on-insulator wafers of 200 mm diameter, 220 nm device thickness and 2 μm buffer oxide thickness are used as the base material for the fabrication. The wafer was pre-diced into square substrates with dimensions of 25x25 mm, and lines were scribed into the substrate backsides to facilitate easy separation into smaller chips once fabrication was complete. After an initial wafer clean using piranha solution (3:1 $\text{H}_2\text{SO}_4\text{:H}_2\text{O}_2$) for 15 minutes and water/IPA rinse, hydrogen silsesquioxane (HSQ) resist was spin-coated onto the substrate and heated to evaporate the solvent. The photonic devices were patterned using a JEOL JBX-8100FS electron beam instrument at The University of British Columbia. The exposure dosage of the design was corrected for proximity effects that result from the backscatter of electrons from exposure of nearby features. Shape writing order was optimized for efficient patterning and minimal beam drift. After the e-beam exposure and subsequent development with a tetramethylammonium sulfate (TMAH) solution, the devices were inspected optically for residues and/or defects. The chips were then mounted on a 4" handle wafer and underwent an anisotropic ICP-RIE etch process using chlorine after qualification of the etch rate. The resist was removed from the surface of the devices using a 10:1 buffer oxide wet etch, and the devices were inspected using a scanning electron microscope (SEM) to verify patterning and etch quality. A 2.2 μm oxide cladding was deposited using a plasma-enhanced chemical vapour deposition (PECVD) process based on tetraethyl orthosilicate (TEOS) at 300°C. Reflectometry measurements were performed throughout the process to verify the device layer, buffer oxide and cladding thicknesses before delivery.

6. Results

6.1. MZI analysis results

For **corner analysis** in Lumerical MODE of the waveguide parameters, I used the design

- ▼ EBeam_LukasChrostowski_MZI.oas_2025051.
- ▶ EBeam_LukasChrostowski_MZI

below.

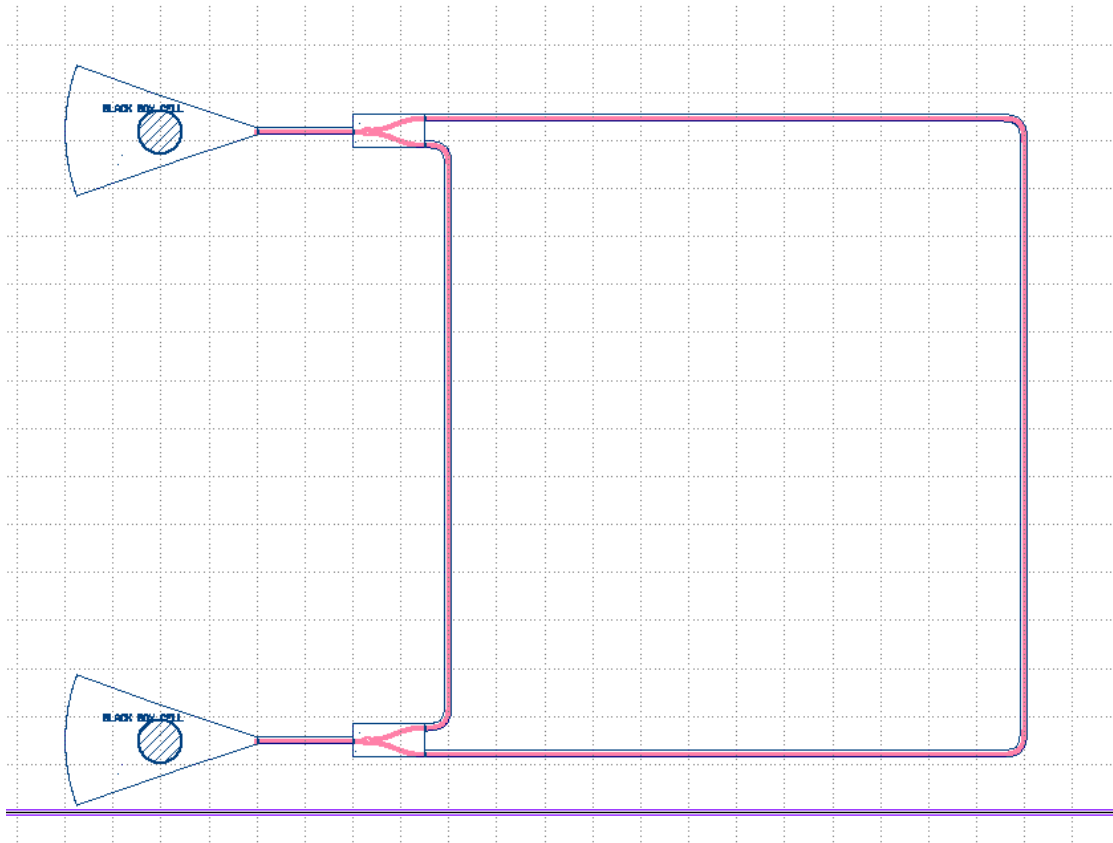


Figure 5: design of unbalanced MZI, the waveguide length difference measured as 251 μm with Klayout.

The first step was to perform an amplitude correction due to spectral distortion caused by Bragg couplers. The correction was performed by a 4th degree polynomial on the results in units of dB. The loss is less than 20dB.

The polynomial coefficients are:

$$P = [-2396234.0 \ 87722.0 \ -15812.0 \ 56.0 \ -24.0];$$

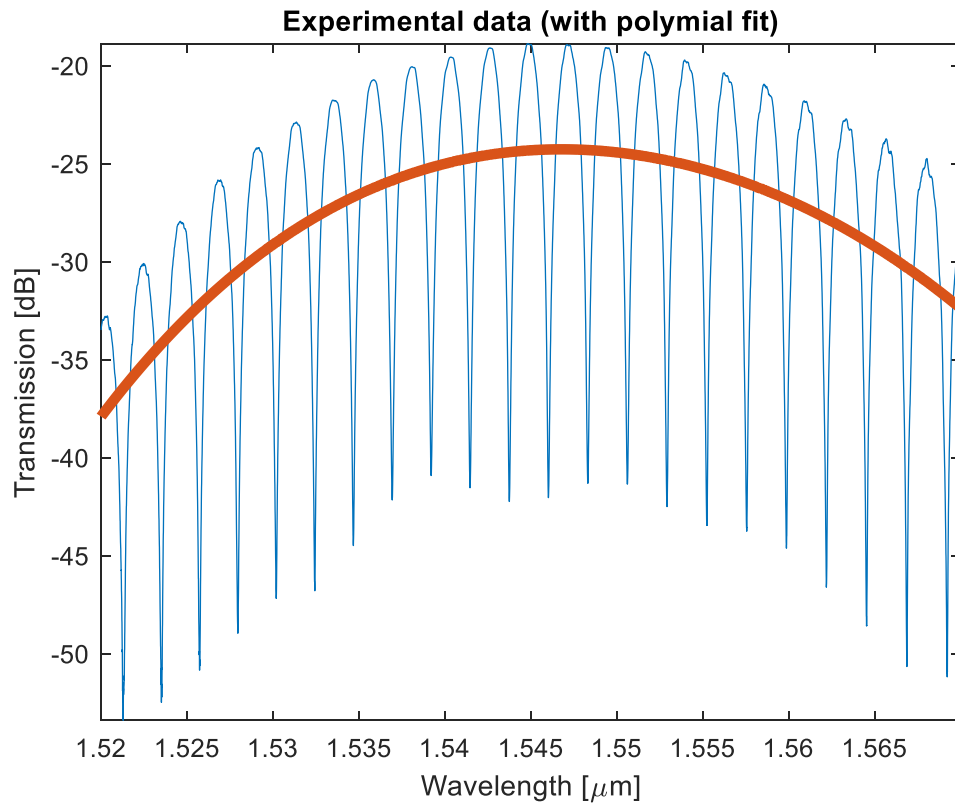


Figure 6: amplitude correction due to spectral distortion caused by Bragg couplers. The correction was performed by a 4th degree polynomial on the results in units of dB. The loss is less than 20dB.

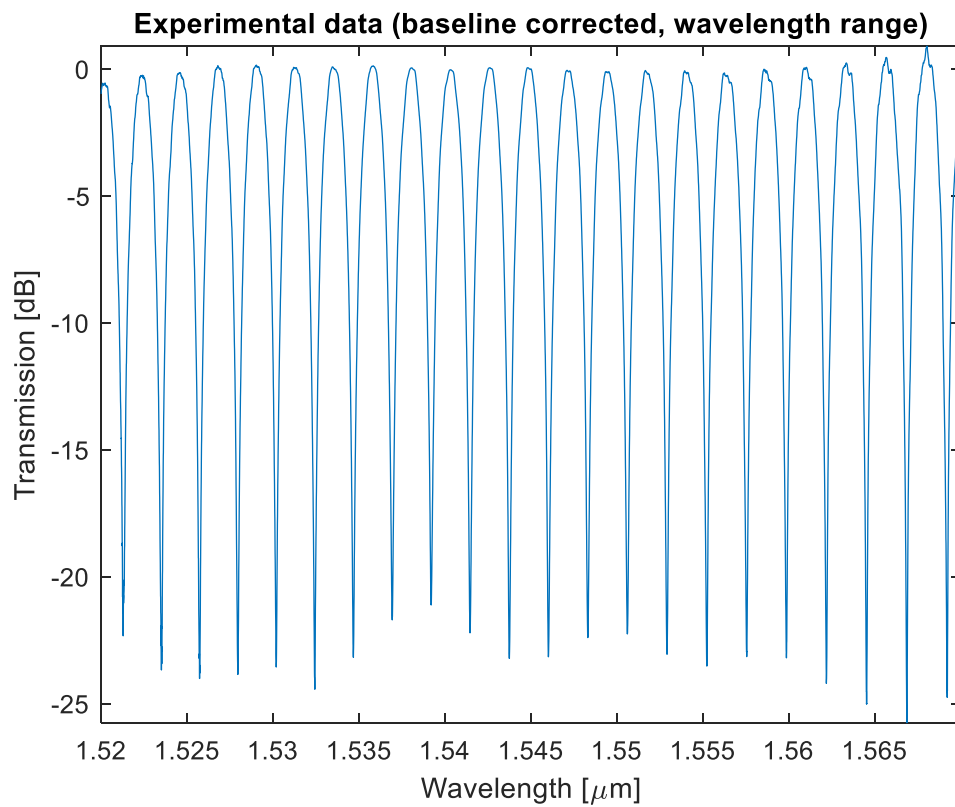


Figure 7: corrected values

The second step is to estimate the period of the interferometer's interference fringes, which is done using the autocorrelation method. Using that estimation to calculate the model parameters.

$$(3) \quad FSR = \lambda_{n+1} - \lambda_n$$

$$(4) \quad n_g = \frac{\lambda^2}{FSR \cdot \Delta L}$$

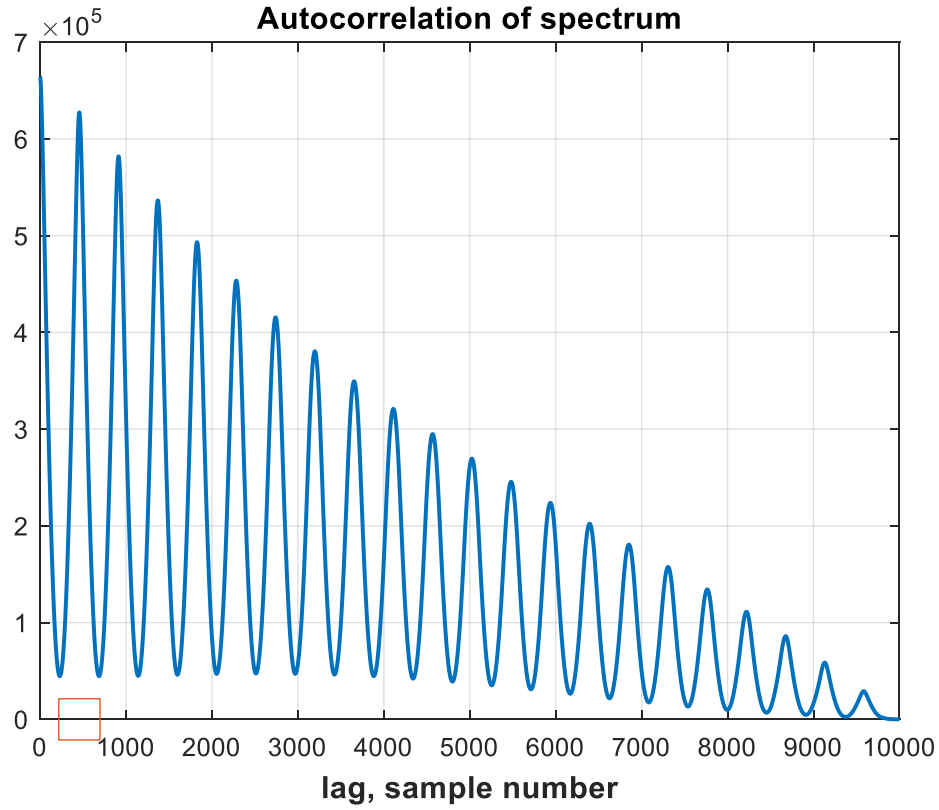


Figure 8: Autocorrelation spectrum of MZI, the lag estimate of the interference fringe cycle is the first peak in the graph marked with a red square. The first peak was located at lag=457, The calculated FSR is 2.285nm and the calculated group index at $\lambda=1545\text{nm}$ is $n_g=4.162$.

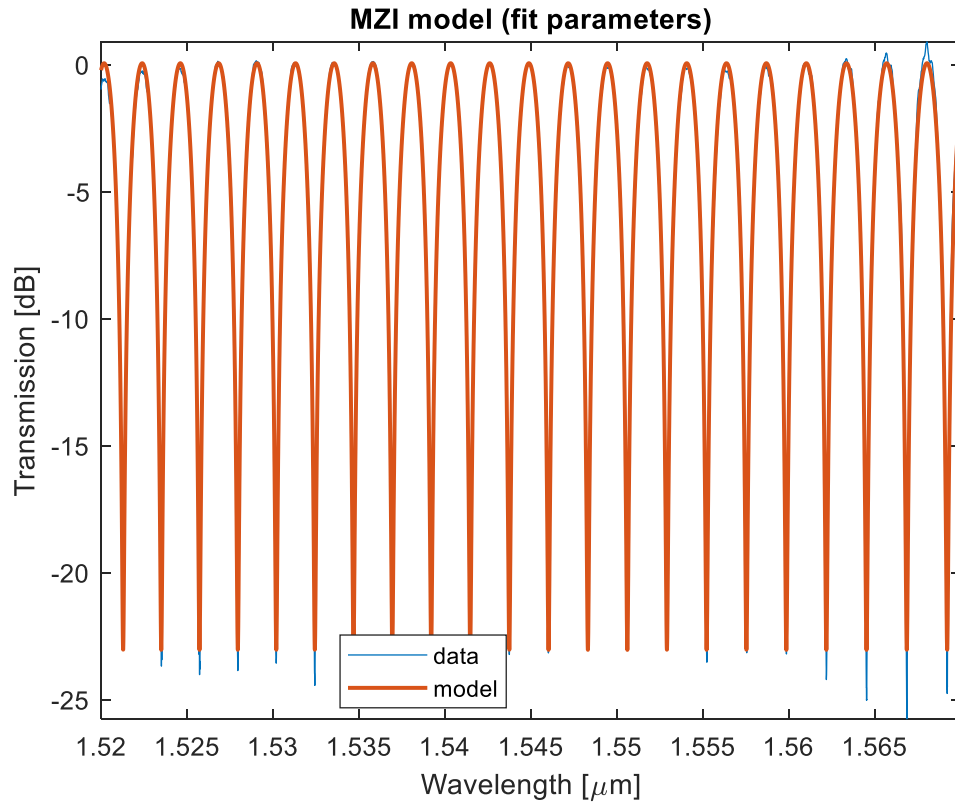


Figure 9: MZI model after fit parameters (red) vs. data (blue)

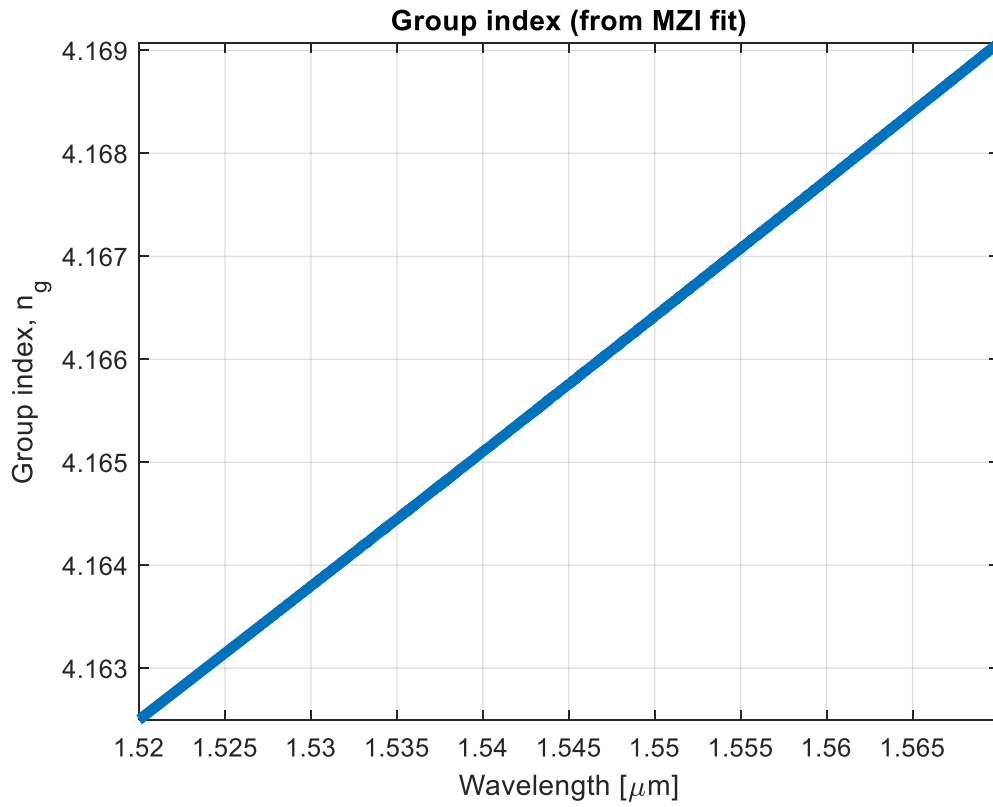


Figure 10: Group index calculated from the fitted model.

6.2. Corner analysis

The effective index and group index were calculated using Lumerical MODE simulation at five different waveguide width and thickness geometries using the Corner Analysis method.

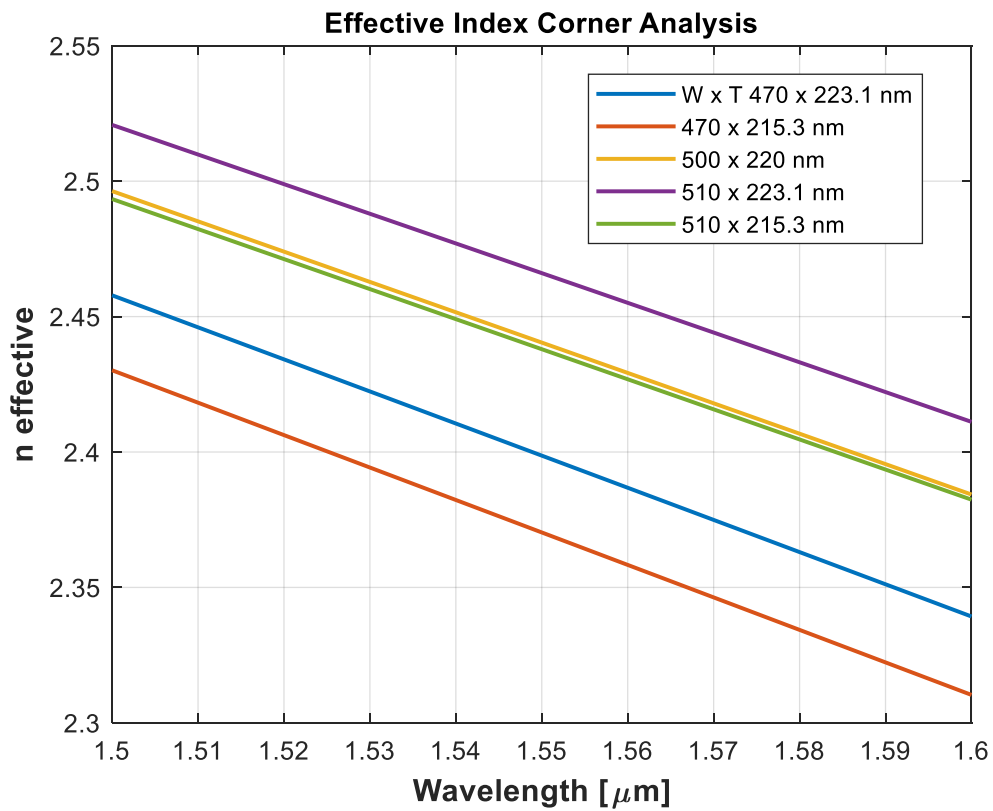


Figure 11: Corner Analysis of the Effective Index.

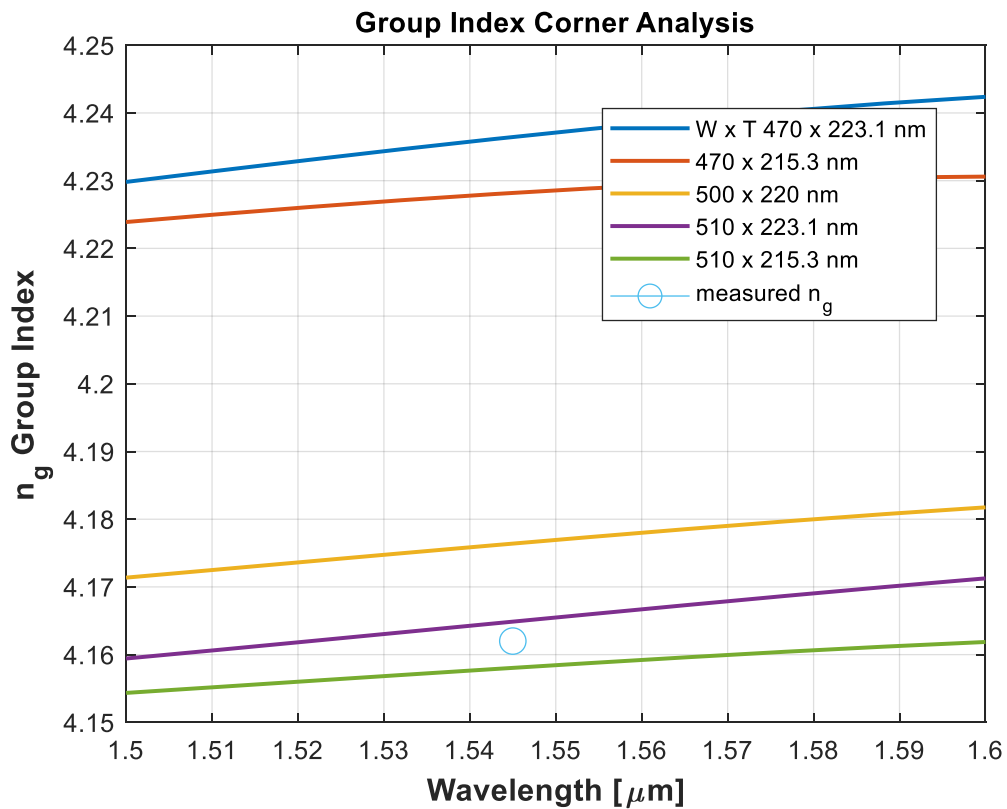


Figure 12: Corner Analysis of the Group Index, the measured group index marked by a blue circle in the graph is located within the limits of the parameters calculated in the waveguide geometries.

6.3. cascade MZI filter analysis results

A phase shift of π is accumulated over a propagation distance of $\frac{\lambda}{2n_{eff}}$ which is of order of 200nm, it is very difficult to control the fabrication process to such precision. Indeed, the measurement results were different from the simulations. In this paragraph, I tried to estimate the errors and assess the reasons for these differences.

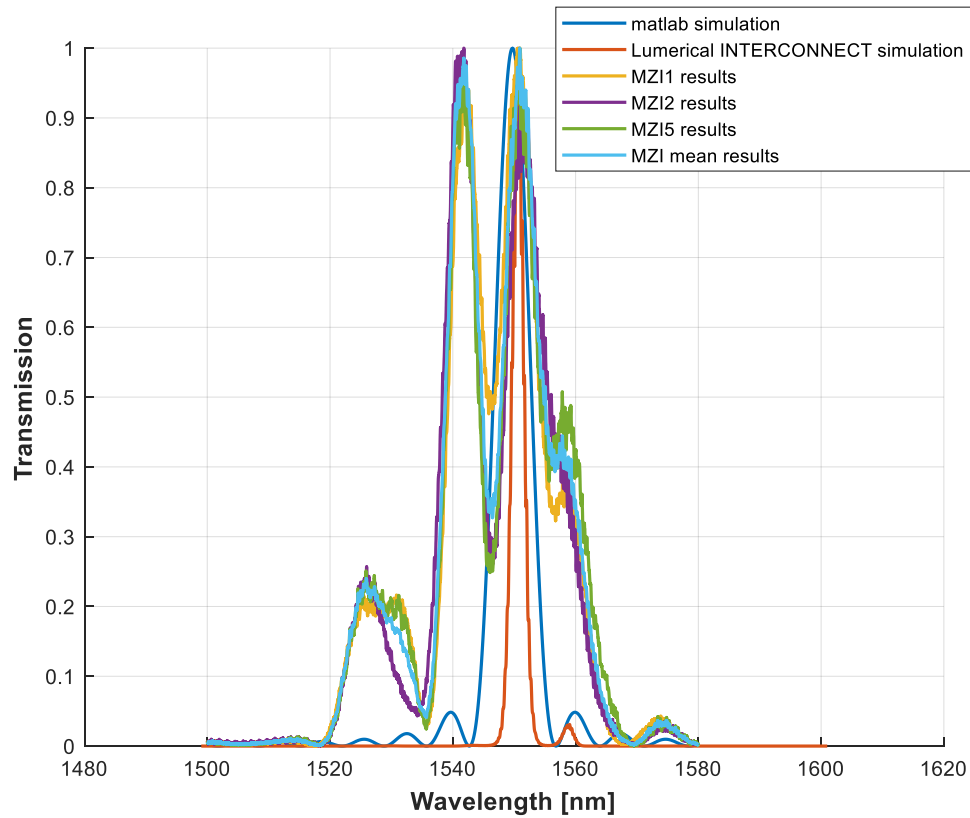


Figure 13: Results of 3 measurements of 4 MZIs in series compared to Matlab and Lumerical INTERCONNECT pre-fabrication simulations.

Error estimation is performed using the least square curve fitting method using Matlab, considering the spectral distortion resulting from the use of Bragg couplers.

```
fun = @(x,xdata) (x(1).*(10.^(p(1)*(xdata - mean(xdata)).^4 + p(2)*(xdata - mean(xdata)).^3 + p(3)*(xdata - mean(xdata)).^2 + p(4)*(xdata - mean(xdata)) + 0)/10))).*(...
    (1+cos(x(2)./xdata.*(x(3)-x(7).*(xdata-mean(xdata))-x(8).*(xdata-mean(xdata)).^2))).*...
    (1+cos(x(4)./xdata.*(x(3)-x(7).*(xdata-mean(xdata))-x(8).*(xdata-mean(xdata)).^2))).*...
    (1+cos(x(5)./xdata.*(x(3)-x(7).*(xdata-mean(xdata))-x(8).*(xdata-mean(xdata)).^2))).*...
    (1+cos(x(6)./xdata.*(x(3)-x(7).*(xdata-mean(xdata))-x(8).*(xdata-mean(xdata)).^2)))));
```

X(3), X(7), X(8) are the Taylor coefficients n_1 , n_2 , n_3 respectively from equation (2). X(7), X(8) were introduced as known constants for silicon $n_2 = 1.13$, $n_3 = -0.001$. n_1 is chosen to

correspond to the deep (zero) depression at wavelength 1549 nm. In variables $X(5)$, $X(6)$, the nominal values of stage 3 and 4 were entered, respectively, according to Table 1. The variables $X(2)$ and $X(4)$ were chosen so that they give the best fit to the model as detailed in Figure 14 and Figure 15.

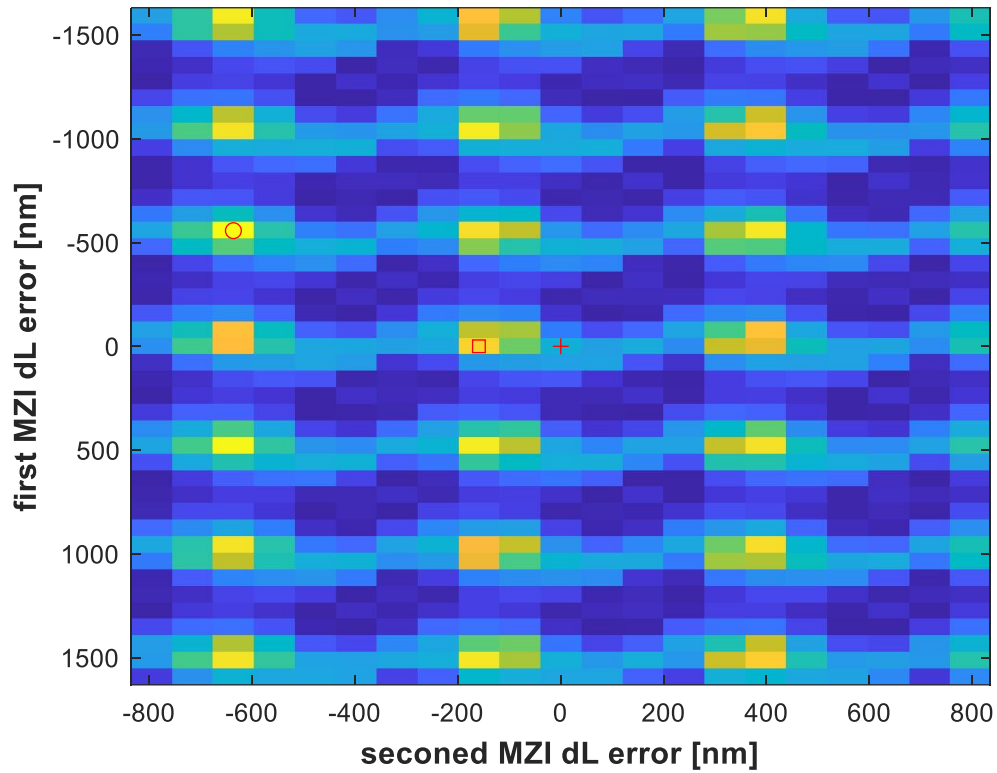


Figure 14: Mapping the estimation quality Q of dL shows the periodic nature of the problem from which the difficulty in estimation arises. In + the nominal value of dL of the first two MZIs in the series, in o the maximum value of Q , in red square the high value of Q near the nominal. The maximum value is far from the probable length error and therefore the closest maximum was chosen.

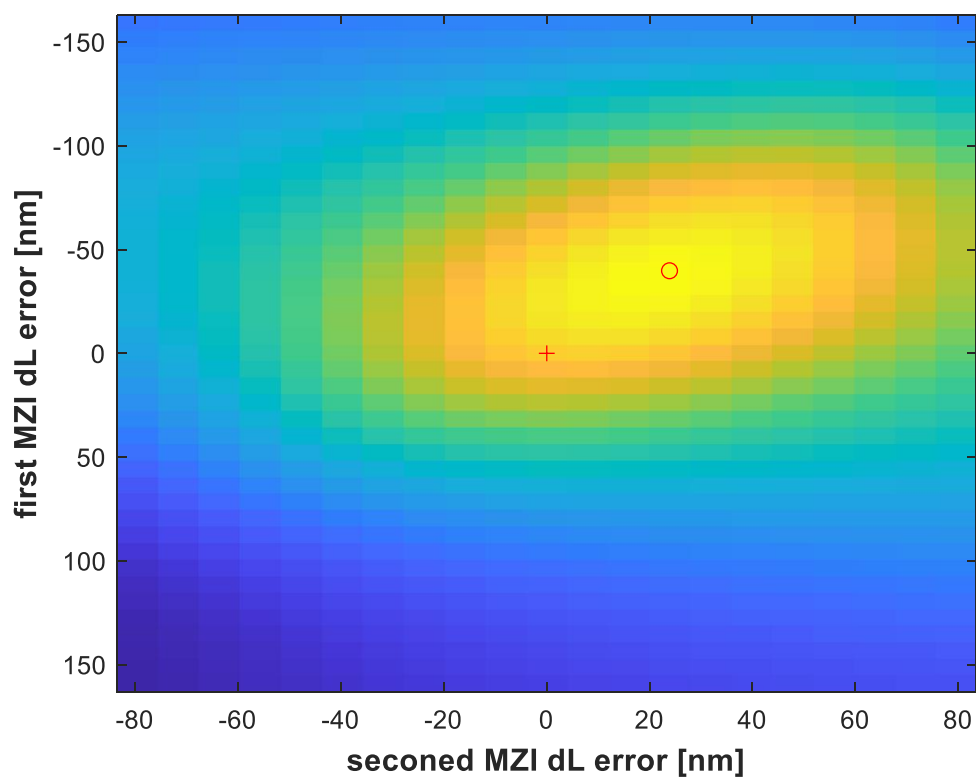


Figure 15: Fine-tuning the error in dL, the peak is obtained at the point (24,-40)nm, $Q = 0.84$.

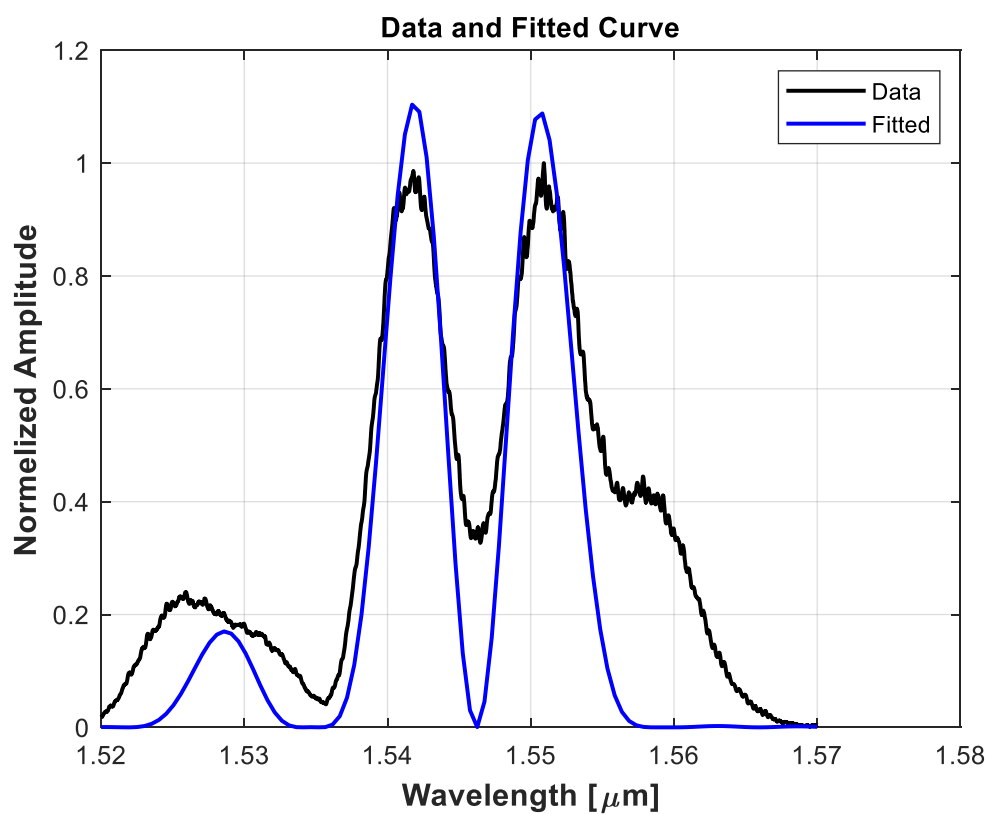


Figure 16: Results mean (out of 3) measurements of 4 MZIs in series compared to Matlab post-fabrication simulations.

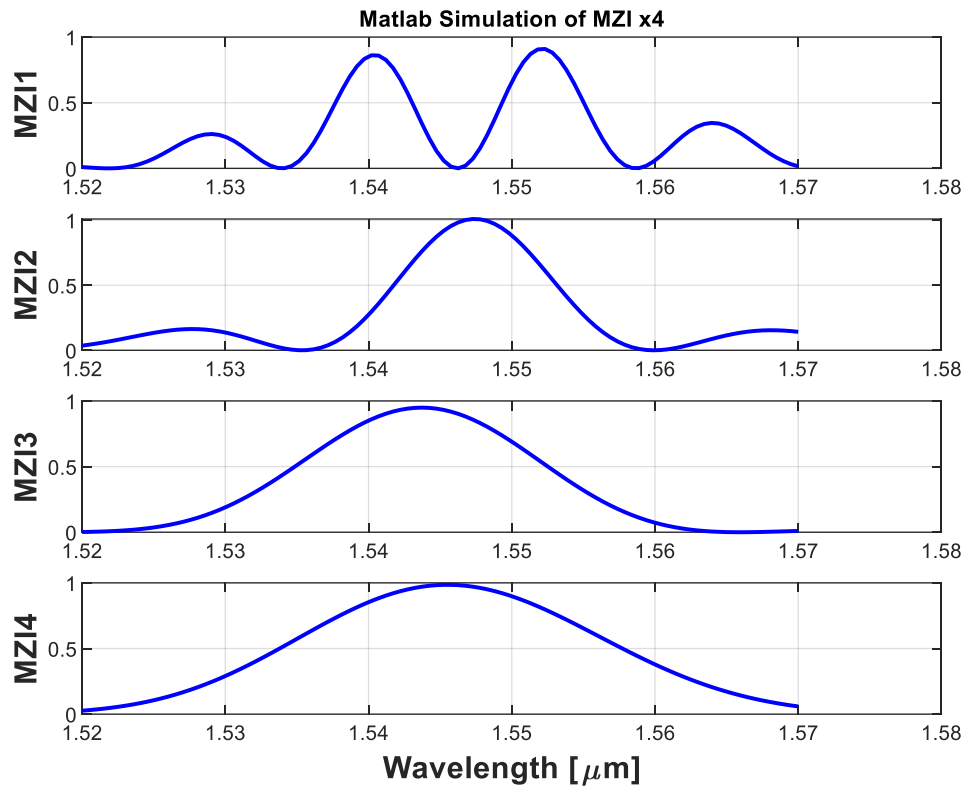


Figure 17: post-fabrication Matlab simulation of the 4 MZI's.

Calculating the cumulative phase with an error of 40 nm

$$\phi_0 = \frac{2\pi}{\lambda} n_{eff} \cdot \Delta L = \frac{2\pi}{1.545} 2.45 \cdot 0.04 = 0.3985 \text{ rad}$$

It is interesting to know whether such an error can be corrected by a heating element in one of the arms of the interferometer.

$$\phi_1 = \frac{2\pi}{\lambda} \cdot \frac{dn}{dT} \cdot \Delta T \cdot \Delta L = \frac{2\pi}{1.545} 1.86 \cdot 10^{-4} \cdot \Delta T \cdot \Delta L$$

$$\phi_0 = \phi_1$$

$$\Delta T \cdot \Delta L = \frac{2.45 \cdot 0.04}{1.86 \cdot 10^{-4}} = 527$$

One can choose $\Delta T = 25\text{K}$, $\Delta L = 20\mu\text{m}$ to solve this problem.

7. Summary and conclusion

In this exercise I used the design and simulation tools Klayout, Lumerical INTERCONNECT, Lumerical MODE and Matlab. cascade 4 filters were designed and manufactured with different delays (8τ , 4τ , 2τ , τ) to receive an overall narrow optical filter. The photonic devices were fabricated using the NanoSOI MPW fabrication process by Applied Nanotools Inc.

From MZI measurements it was found that the calculated FSR is 2.285nm and the calculated group index at $\lambda=1545\text{nm}$ is $n_g=4.162$. The group index value is in the range of group indexes that were calculated in the Corner Analysis.

The measurement results of the 4-MZI series were compared to the expected model using the least square method. From the comparison, it was concluded that the discrepancy with the simulation stems from a difference in the waveguide length of about 40 nm. This error can be corrected, for example, by heating one of the arms of the interferometer in future work.